Trip and history-based range prediction for a light powered vehicle based on real-world data

David Martins Neto
david.neto@tecnico.ulisboa.pt

Instituto Superior Técnico, Lisboa, Portugal

September 2020

Abstract

The present work focuses on alleviating the range anxiety in the context of electric vehicles using real world-data collected in a light powered vehicle. To do this, the original lead-acid battery pack of the vehicle was changed into lithium-ion, achieving a 25% gain in autonomy. A data acquisition system was also developed and integrated with the new battery pack recording global position data from a GPS receiver and battery information from the Battery Management System (**BMS**). The data collected was then used to test trip and trip-based methods to alleviate range anxiety. The history-based methods used both physical and statistical models to predict the energy consumption of varying duration trips. In the physical models the best results were obtained with the regression, which achieved 3% average error and 13% error standard deviation, for 150s segments. From the statistical models the best results were obtained with the decision tree regression with a 1% average error and a 26% error standard deviation, for 150s segments. The history-based methods used moving averages to predict the remaining driving range of the vehicle. In this work, the moving average was made in a constant time window as well as in a constant distance window. For a constant time window of 2h45min it was obtained a 8.1% mean error with 19.7% standard error deviation. For the constant distance window of 80km it was possible to obtain a average error of 2% and a standard error deviation of 8.2%. s

Keywords: electric vehicles, BEV, smart mobility, range prediction, vehicle modelling, data science.

1 Introduction

Following the 2016 Paris agreement, 195 countries formulated the commitment of keeping the global temperature rise below the 2 degree mark. In order to that, the greenhouse gas emissions have to decrease drastically. As responsible for one fourth of the CO_2 emissions[1], the transportation sector will need to go through profound changes. This requires the shift from the widespread internal combustion engine (ICE) into the electric vehicles (EV), which make use of electric engines to provide the propulsion energy. From the EV's, the most effective in reducing emissions are the battery electric vehicles (BEV). These vehicles are completely electric and have zero tailpipe emissions.[2].

Light powered vehicles such as motorcycles and small three-wheelers such as the one used in this work are of particular importance in the road to widespread vehicle electrification. They are often urban vehicles and travel shorter distances at lower velocities. They are also smaller than other vehicles. Because of this, they have smaller energy consumption and require smaller battery packs[2], which in turn makes its electrification easier.

1.1 Range Anxiety

Despite the improvement of the vehicle technology, the vehicle range still ranks as one of the three most important costumer concerns over BEV purchase[3]. Range anxiety can be defined as the fear that the driver has of not being able to reach the destination because of the finite range of the vehicle [4]. This effect arises from the mismatch between the costumer vehicle usage and the vehicle range.

One way of solving the range anxiety problem is to provide the driver with accurate information about the vehicle consumption and the available range. In order to do this, there can be taken two major approaches[5]. The **trip-based** and the **history-based** methods.

1.2 Trip-Based Methods

The first way to eliminate range anxiety is through early planning of the vehicle using a rout-planner. For a known route, the total energy consumption can be predicted using different models. The problem is formulated by equation 1, where ΔE is the

total energy spent in a trip, x_i are trip features such as the distance travelled, average velocity etc., and f_j can represent any of the models used. These methods are often called **trip-based** and have been shown to reduce range anxiety[6].

$$\Delta E = f_j(x_1, ..., x_n) \tag{1}$$

The models (f_i) used in these methods are often divided into physical and statistical models. The former attempts to provide the most accurate vehicle representation by using physical laws to describe each part of the vehicle. The latter, instead combines statistical methods and measurements form the vehicle to provide an accurate description.

1.2.1 Physical Model

There are several studies made using physical models of the vehicle[7–14] to estimate the energy consumption. In figure 1, a simplified representation of the battery-to-wheel energy flow in a fully electric vehicle is shown. It can be seen that, as the energy flows from the batteries to each of the vehicle components,there are losses in energy. In the present work, the auxiliary power is discarded because its contribution is small when compared with the other terms.

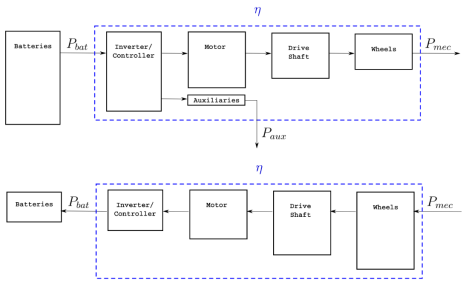

Figure 1: Energy flow scheme battery-to-wheel(above) and wheel-to-battery(below). The size of the box is a visual indicator of the relative power reaching each component.

As shown in figure 1 the efficiencies of the inverter, the controller, the motor and drive shaft were grouped in a single value. The efficiency is then given by equation 2, where P_{mec} is the mechanical power and P_{bat} is the battery power.

$$\eta(T, \omega) = \frac{P_{mec}}{P_{bat}} \tag{2}$$

Of the components in the vehicle, the one that will affect the consumption the most is the motor. The electric motor changes its efficiency significantly depending on the torque and rotational frequency.

As seen in equation 2, the power measured in the batteries is proportional to the mechanical power (P_{mec}) provided to the vehicle. The most common physical model to predict this power is the lumped mass model. There are three main forces considered in this model: the gravitational force (F_g), the rolling friction (F_r), the aerodynamic friction (F_a), and to balance them, the traction force (F_t) applied by the motor. A schematic representation of these forces is shown in figure 2.

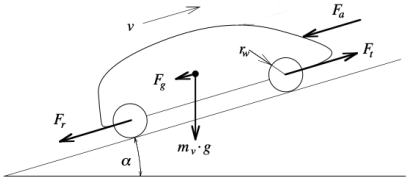

Figure 2: Graphical representation of forces acting on the vehicle adapted from [15]. (F_t - traction force, F_r - rolling friction, F_a - aerodynamic friction, F_g - gravitational force)

Introducing this forces in Newton's second law of motion, it is possible to obtain the main equation of the model shown in equation 3, where m is the vehicle mass and $v(t)$ is the velocity of the vehicle[15].

$$m\frac{d}{dt}v(t) = F_t(t) - (F_a(t) + F_r(t) + F_g(t)) \tag{3}$$

The aerodynamic force is given by 4 where ρ is the air density, C_D is the aerodynamic drag coefficient and A_f is the frontal area of the vehicle.

$$F_a = \frac{1}{2}\rho A_f C_D v^2 \tag{4}$$

The rolling friction is given by equation 5, where m is the mass of the vehicle, g is local gravitational field of Earth and α is the slope of the road. c_{r0} is the rolling coefficient and Q, an empirical constant defined to be $44.4m/s$.

$$F_{roll} = m \cdot g \cdot cos\alpha \cdot c_{r0} \cdot \left(1 + \frac{v}{Q}\right) \tag{5}$$

The gravitational force is given by equation 6, where m is the mass of the vehicle, g is local gravitational field of Earth the and the α is the slope of the road.

$$F_g = m \cdot g \cdot sin\alpha \tag{6}$$

From the previous formulation of the lumped mass model, the ΔE is the integral that can be expressed as shown in equation (7).

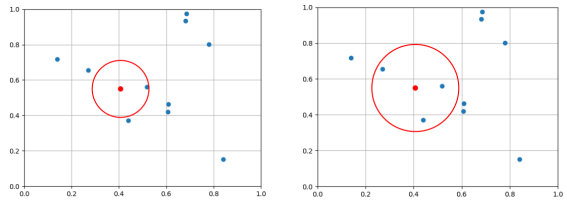

(a) $K = 1$ (b) $K = 3$

Figure 3: Points in the training set (blue) that are used in the weighted average prediction of the unknown point (red) for three different values of K.

$$\begin{aligned}\Delta E = & \underbrace{\frac{1}{2} m \cdot (v_f^2 - v_i^2)}_{\text{Kinetic Energy Variation}} \\ & + \underbrace{c_r \cdot m \cdot g \left(\Delta s_{xy} + \int_{x_i}^{x_f} v \cdot dx \right)}_{\text{Rolling Friction Energy Dissipation}} \\ & + \underbrace{m \cdot g \cdot \Delta h}_{\text{Potental Gravitational Enrgy}} \\ & + \underbrace{\rho \cdot c_D \cdot A_f \cdot \int_{x_i}^{x_f} v^2 \cdot dx}_{\text{Aerodynamic Friction Energy Dissipation}}\end{aligned} \tag{7}$$

1.3 Statistical Model

In addition to physical models, statistical models have also been used to estimate the energy consumption of road vehicles. These models do not require the knowledge concerning the physical mechanisms at play in the vehicle motion or any types of parameters which characterise it. In previous studies, models including neural networks[16–18], decision trees[17] and K-nearest neighbours[19] have been used. The way that these methods work is by using data to build a model that describes them well without any knowledge of the physics involved. Statistical models should improve as the data collected increases, allowing them to capture finer details of vehicle consumption behaviour.

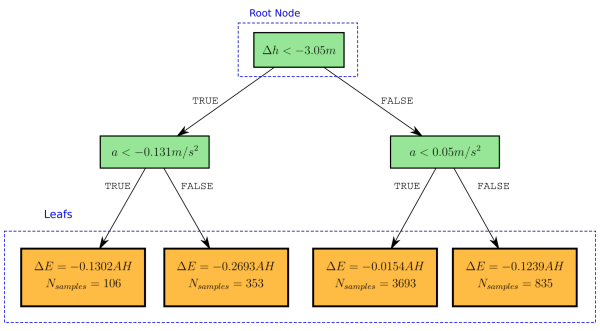

Figure 4: Decision Tree Example

1.3.1 K-Nearest Neighbours

The way this algorithm works is, when presented with a new data point, it will compute the distances between that point and the ones in the training data. The energy prediction will then be a weighted average of the energy measured in the K points that are closest from the new one. This is the reason for the name K-nearest neighbours. In figure 3, three examples of the algorithm working in a data set for several values of K can be seen. As it is possible to observe the points in the training set (blue) are used in the weighted average prediction of the unknown point (red) for three different values of K.

1.3.2 Decision Trees

In order to better understand the decision tree models a simple example taken from the data collected is provided in figure 4, where Δh is the height variation from the trip start to finish, a is the average acceleration and ΔE is the total energy spent in the trip. As one can notice, the decision tree can be pictured as a graph where each of the nodes represents a binary decision based on the data features. In order to make the energy consumption prediction successive tests are made to the data, staring at the root node and following the chart all the way through until the leafs are reached. In order to generate this trees from the data the algorithm used was the CART algorithm[20].

1.4 History-Based Methods

The second way of alleviating range anxiety does not involve early planning of the trip. It uses instead only the past consumption of the vehicle to predict the future behaviour. Because of this, they are called **history-based** methods. They often are less accurate than the trip based methods mainly because they do not have access to the road topology, which is one of the most determinant factors in the vehicle consumption.

There are also several studies concerning history-based methods in literature, where the most common way of estimating the vehicle consumption is through the usage of a moving average. [21–23]

In this work different types of range prediction methods were implemented. The trip- based prediction was implemented using three different regression methods (Decision Tree, K-Nearest Neighbors, and Linear regressions) and the history-based predictions us- ing two different ways to choose the window of past values (constant time and constant dis- tance).These methods were evaluated using experimental data spanning over 300km in Lis- bon city center. The vehicle used was a electric light three wheel vehicle (category L).

1.5 Objectives

The present work can be divided into three different parts. The first part was the conversion of the battery pack of the vehicle used from the original lead-acid batteries to new lithium-ion batteries. This involved the modification of the previous battery pack to hold the new batteries as well as devising the new wiring of the previous batteries.

The second part of the work consists in building the data acquisition system in order to collect and log important features in the course of the vehicle movement. In general, the information regarding the battery pack will be collected from the Battery Management System (BMS) and combined with information regarding the vehicle position from a GPS receiver using a *Raspberry Pi*.

In the final part of the work, the data collected will be analysed and used to test different methods of solving range anxiety. Both trip and history-based methods are tested, using in the first several physical and statistical methods and in the second a moving average based method.

2 Data Collection

This work is focused in a fully electric three-wheel light powered vehicle, commonly knwon as *auto rickshaw*. The vehicle studied in particular was a **e-tuk Limo GT** model manufactured by e-tuk Factory and can be seen in figure 5. The battery bank of the e-tuk consisted of 24 160 Ah batteries, with a nominal voltage of 76.8V. The motor in this vehicle was a 7kW three phase AC motor.

Figure 5: **e-tuk Limo GT**

2.1 Battery Conversion

In the present work the battery pack of the vehicle was successfully converted from the original lead-acid batteries to a new $LiFePO_4$ lithium-ion pack. After the battery pack conversion, it was achieved a increase of 25% in the vehicle range, relative to the one provided by the manufacturer. It is also expected the increase in the durability of the batteries to 2000 cycles in stead of the previous 600, which corresponds to a 230% increase in durability.

In order to do this, a new battery compartment was designed to hold the now smaller and lighter batteries in place. The full view of the battery pack can be seen in figure 6.

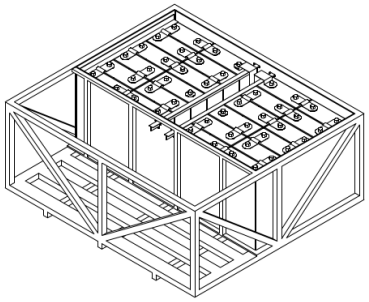

Figure 6: Isometric view of the assembled battery compartment.

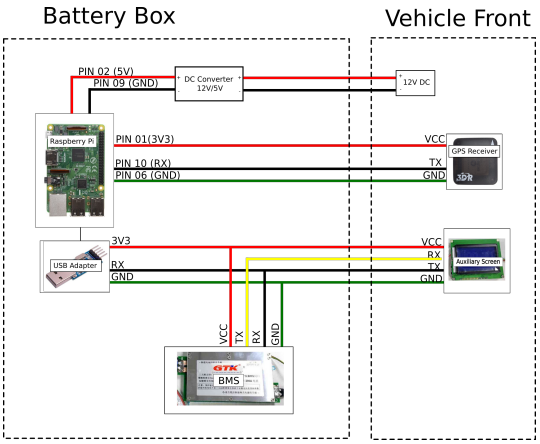

Figure 7: Schematic of the wiring in the main set-up used.

2.2 Data Acquisition System

A data acquisition system was developed and tested to log the geographical position of the vehicle as well as information concerning the battery pack. The geographical information contained latitude and longitude of the vehicle vehicle as well as the velocity of the vehicle. The battery information contained the battery pack voltage, current, SOC, power etc.. This system was done using a *Raspberry Pi* connected to a GPS receiver and also to the BMS through serial communication. The set-up was tested using a **e-max** motorcycle and adapted to fit the new battery pack of the *e-tuk*. The software used to make the data acquisition was developed in *Python*, within object oriented programming. For each individual acquisition one individual class was used. It was also implemented a webpage hosted in the *Raspberry Pi* to read the last point recorded without need for connection via SSH.

3 Derived Data

The collected data was mostly used in the future models, but there were two features that needed to be estimated, which were the distance and the altitude. In the last section it is shown the estimation of the efficiency map of the drivetrain.

3.1 Altitude

Despite having access to the altitude data provided by the on-board GPS receiver, the accuracy of these measurements was not sufficient for the usage in vehicle modelling. Because of this, altitude data of Lisbon city centre was obtained through *Mapbox*, using their *Mapbox Terrain-RGB* API in *Python 3*. This API uses the altitude taken from the *Copernicus* EU project, which derives its data from a weighted average of the *Shuttle Radar Topography Mission* (SRTM) and *Advanced Spaceborne Thermal Emission and Reflection Radiometer* (ASTER). Both of these datasets have smaller area resolution and provide one altitude measurement for every 30 meters (square of area $900m^2$). Despite not being ideal, this is the only one available for free use.

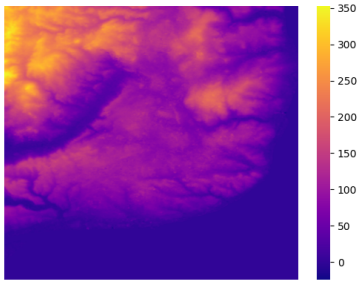

Figure 8: Elevation map of the Lisbon Area taken from *Mapbox Terrain-RGB*

3.2 Horizontal Distance Estimation

The GPS receiver measures the sequence of locations of the vehicle. The location is given by a pair of values (λ, ϕ), where λ represents the latitude and ϕ represents the longitude. The distance between two successive points was determined using equation (8). Where E_R represents the *Earth Radius*, which was considered to be equal to $6371008.8m$, and λ_m represents the average latitude of the two points. As the points are most of the times very close together, there will not be a very large difference in latitude, and the approximation will be valid.

$$\Delta s_{xy} = E_R \sqrt{\Delta\lambda^2 + (\cos\lambda_m \cdot \Delta\phi)^2} \tag{8}$$

3.3 Drivetrain Efficiency Estimation

The previous model considered only the physical properties of the vehicle. However, it is known that the motor efficiency changes prominently depending on the operation point of the motor. To characterise the efficiency of the motor it is common to use the efficiency map. This map is often represented as a function of the torque and velocity acting on the motor.

Unfortunately, no data concerning the efficiency of the motor of the vehicle was not provided by the manufacturer. Nevertheless, using the *a priori* model described in the previous section it was possible to estimate the mechanical power on the wheels, using equation 9, where F_t is the traction force given by the lumped mass model as shown in equation 3.

$$P_{mec} = v \cdot F_t \tag{9}$$

The acceleration was estimated using a linear regression to the previous three seconds of velocity values and extracting its rate of change. This was also done to estimate the slope although now estimaing the value of $\tan\alpha = \frac{\Delta h}{\Delta s_{xy}}$. The values of velocity used were the instantaneous measured by the GPS. and finally the vehicle parameters used are shown in table 2.

To build the efficiency map, the values of P_{mec} as well as P_{bat} were split in two dimensional bins as a function of their torque and velocity values. The values of the efficiencies were averaged inside the bins to build the two dimensional map that can be seen in figure 9.

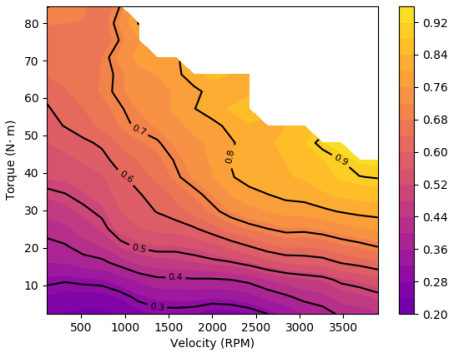

Figure 9: Different Representations of the efficiency map of the motor.

The general form obtained for the drive-train efficiency map is similar to the motor efficiency. This is to be expected because the motor is the most important component in the drive-train. Because of inaccuracies in the individual height measurements, it was not possible to find the values of the individual power consumption using this model and then the integrated energy consumption could not be used in the trip-based methods described in section 4.

4 Trip-Based Prediction

The **trip-based** models implementes were evaluated using the R^2 metric given equation 10.[24]. For

the physical models the R^2 value presented is obtained considering all the points in the dataset. To evaluate the statistical models the K-Fold cross validation method with 10 folds was used.

$$R^2 = \frac{\sum_i (y_i - f_i)^2}{\sum_i (y_i - \bar{y})^2} \tag{10}$$

4.1 Physical Models

In table 1 the data used as input for the physical models can be seen. This data is relative to fniite trip segments.

Feature Name	**Expression**
Variation of the velocity Squared	$(v_f^2 - v_i^2)$
Total Height Variation	Δh
Total Distance Travelled	Δs_{xy}
Velocity Integral	$\int_{x_i}^{x_f} v \cdot dx$
Velocity Squared Integral	$\int_{x_i}^{x_f} v^2 \cdot dx$

Table 1: Features used and respective expressions in the physical models.

4.1.1 *A priori* Physical Model

This model is based on the **lumped mass model** described ipreviously and takes the form of equation 7. The parameters used in this section are some typical values expected for a vehicle of this type that can be seen in table 2, where both the rolling and aerodynamic coefficient were taken from the model developed in [11], and the vehicle mass was estimated estimated from manufacturer data.

Name	**Symbol**	**Expected Value**
Drag Area	$C_d \cdot A$	$1.75m^2$ [11]
Rolling Coefficient	c_r	0.012 [11]
Vehicle Mass	v_m	1000 kg

Table 2: Coefficients for the vehicle in study

4.1.2 Regression Model

The first logical step towards improving upon the *a priori* model is to try to provide better estimations for the model parameters. Using the general equation of the lumped mass model described before a least squares regression to the data collected and determine the model parameters that are better suited to describe it.

The first model (**model 1**) did not consider the aerodynamic friction or the dependence of the velocity of the rolling friction. The second model (**model 2**) adds the effect of the *aerodynamic friction* acting on the vehicle. The third model (**model 3**) considers the effects of both the aerodynamic friction and the velocity term of the rolling friction.

Parameter	Value
m	959 kg
c_r	0.04
$C_d \cdot A_f$	1.24 m^2

Table 3: Vehicle Model Parameters for a segment size of ($R^2 = 0.95$)

In table 3 it can be seen examples of the vehicle parameters obtained in the regression model. In can be seen that the rolling friction coefficient is much higher than it would be expected for rolling coefficient of wheels rolling over concrete, which were expected to vary form 0.010 to 0.015. This can be explained by the fact that the vehicle does not move in concrete for a lot of its travel time. The other two values are inside the expected for a road vehicle.

4.2 Statistical Models

In this section two different data-driven statistical models were implemented: the decision tree and KNN regression models. The implementation used the *sklearn* Python libraries and for training used the same aggregated trip data shown in table 4. For both statistical models it is made a hyperparamenter optimization. In the following sections the parameter configuration that provided the best results is shown.

Feature Name	**Expression**
Average Acceleration	$\frac{1}{N}\sum_i a_i$
Velocity Squared Integral	$\int_{x_i}^{x_f} v^2 \cdot dx$
Average Trip Velocity	$\frac{1}{N}\sum_i v_i$
Total Distance Travelled	Δs_{xy}
Total Height Variation	Δh
Trip Duration	Δt

Table 4: Features used and respective expressions in the statistical models.

4.2.1 Decision Tree Regression

The final parameters chosen for the decision tree used were a maximum depth of 4,and the default values of 2 and 1 for the minimum number of samples per split and minimum samples per leaf, respectively were chosen.

4.2.2 KNN Regression

For the final KNN model, 40 neighbours were considered, using uniform weights and the euclidean distance metric.

4.3 Model Comparison

In this section we compare the results obtained for the different implemented models, and provide a

discussion of the pros and cons of using each model as well as a summary of the main conclusions. The grouped results obtained can be seen in figure 10.

The most striking difference between the data-driven models (*KNN* and *Decision Tree*) and the physics-based models (*a priori* and regression models) is that for longer trip segments the data-driven models start to fail. This happens because, as said before, the larger the trip segment the smaller the dataset, and the dataset becomes smaller than the necessary for the model to make accurate predictions. On the other hand, the physics-based models already have the information of the vehicle model and can more easily generalise from smaller datasets.

From the data-driven models we can see that the decision tree model provided the best performance. From the physics-based models, the one that provided the best results were the regression models, with small differences between the models. But the *a priori* model showed the best results for the smaller trip segments, where the regression models could not find the accurate model parameters to describe the vehicle.

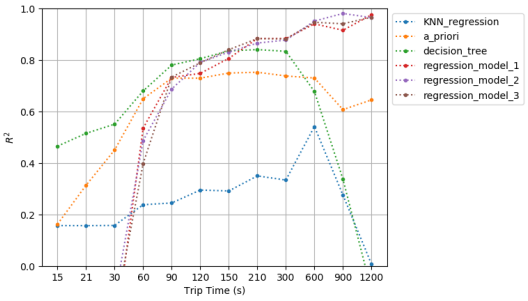

Figure 10: Joint Representation of the R^2 for all the models that were used to describe the vehicle

Table 5 is a compilation of average errors and standard error mean deviation data for the different models. We can see that the standard deviation of the error closely follows the performance expected by the R^2 value of the models. However, it is possible to see that that is not quite the case for the bias. It is observed that the model which has the most (absolute) bias, with 32%, is the *a priori* model, followed by the KNN model, with 7%. The model that had the less bias was the decision tree model, despite the fact that the R^2 value was higher than the regression model.

5 History-Based Methods

In contrast to the previous section, the focus of this chapter is to implement and test, using the real-world data collected, a system that allows the estimation of the vehicle range without the knowledge of the future vehicle trajectory. This was done using a **moving average**. The general form that a moving average takes can be seen in equation 11, where the y_t are the values that the series takes for time t, and N is the length of the moving average window [25].

Model	Average Error (%)	Standard Deviation (%)
Regression Model	3	13
A priori Model	-32	27
KNN	7	52
Decision Trees	1	26

Table 5: Average and standard deviation of the error values for the different methods.

$$MA_i(y) = \frac{y_t + y_{t-1} + ... + y_{t-(N-1)}}{N} \tag{11}$$

In this particular case, we want to estimate the consumption per distance travelled by the vehicle ($\bar{p}$). In order to do that, two moving averages are computed as shown in equation in equation 12, where $MA_i(I)$ and $MA_i(\Delta s)$ represent the moving average values for time t of the current consumed and the distance travelled by the vehicle, respectively. Both of the moving averages are computed in the same way and for the same window. the computation of the average consumption allows us to then estimate the remaining driving range (RDR) of the vehicle using equation 13, where SOC_t is the instantaneous state of charge in the battery provided by the BMS, and the f_{cal} is a calibration factor.

To estimate the calibration factor we compute for all of the trips collected the distance travelled (Δs_{trip}) and the range variation ($\Delta RDR_{trip} = RDR_i - RDR_f$) from start to finish. This calibration factor is then estimated using a linear regression to equation 14. An example of a calibration is shown in figure 11.

$$\bar{p}_i = \frac{t_w \cdot MA_i(I)}{MA_i(\Delta s)} \tag{12}$$

$$RDR_i = \frac{SOC_i}{\bar{p}_i} \cdot f_{cal} \tag{13}$$

$$\Delta RDR_{trip} = f_{cal} \cdot \Delta s_{trip} \tag{14}$$

To test the history based models, the range was calculated for the entire day of data acquisition of the vehicle. For each of this estimations the error was computed using equation 15. The average error as well as standard deviation of the errors of the predictions were the main evaluation metrics considered.

$$e = \frac{\Delta RDR - \Delta s}{\Delta s} \tag{15}$$

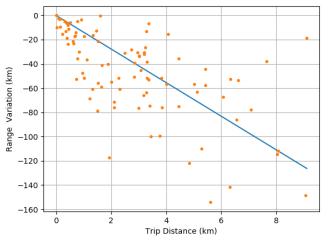

Figure 11: Example of a graph of the calibration

This tests were used in the following two sections, which consider two ways of choosing the moving average. The first corresponds to the constant time window and the second to the constant distance window.

5.1 Time Window

The range prediction was made over all the charging cycles that were acquired for varying time windows. The average value of R^2 obtained can be seen in figure 12 as a function of the time window considered. It is possible to see that for the points **with calibration** the R^2 approaches 1 for windows above 10000 s (around 2:45 h), which indicates that this is the minimum value for a correct description of the measured data.

From the values of errors for the charging cycles, it was computed the average error and the standard deviation of the values. In figure 13 it can be seen the evolution of the average error as well as the evolution of the standard deviation of the errors. As seen before the values tend to stabilise for bigger time windows, as the bigger the window the less the values will vary.

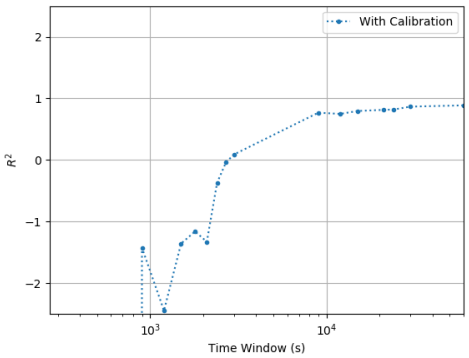

Figure 12: Evolution of the R^2 as a function of the window used.

5.2 Distance Window

The evaluation of the model was made in the same way as for the **time window** models. For this model, the results also improved upon calibration. Because of this the data presented corresponds only to calibrated data. In figure 14 it can be seen that the value of R^2 once again stabilizes close to one for widows above 30 kilometres. However, as can be seen in figure 15 the average error is still considerable and only becomes close to zero for windows of around 80 km. For these bigger windows, it can be seen that the standard deviation of the error is close to 10%, which is a acceptable value.

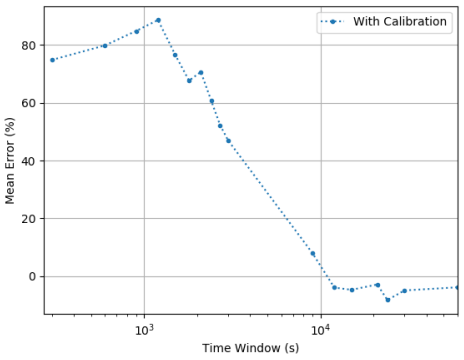

Figure 13: Values of the mean error and standard deviation of the error values for various time windows.

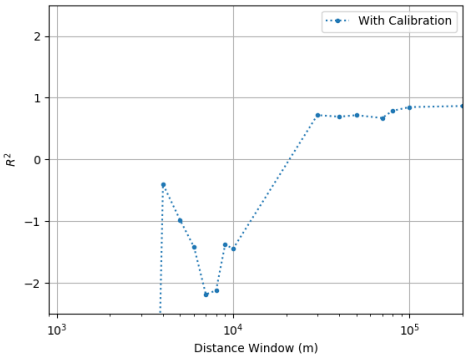

Figure 14: Evolution of the R^2 values for the constant distance window moving average as a function of the window considered.

5.3 Model Comparison

The objective of this section was to determine which of the ways of choosing the window produced the best results for this real time methods. We make this by comparing the best results obtained with the constant time window to the best ones obtained using the constant distance window. Table 6 shows the R^2 average and standard deviation for both models. It is verified that both values are relatively close to one another. Both present an acceptable fit

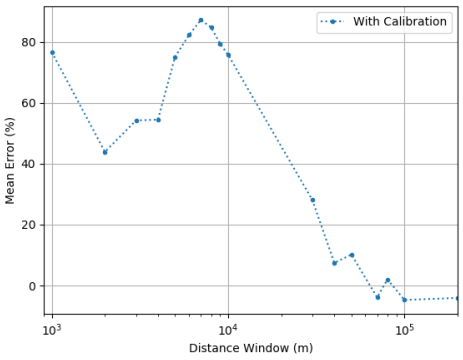

Figure 15: Examples of the range prediction profile for two different time windows.

to the measured data and the results show consistency across the different days considered, showing a relatively low standard deviation. In table 7 it can be seen the mean and the standard deviation of the relative error for the cycles considered. It can be seen that the distance window method showed itself to be more accurate with a lower average error, as well as more precise with a lower error standard deviation.

Window	**Mean** R^2	**Standard** R^2 **Deviation**
$t_w = 2:45min$	0.77	0.13
$d_w = 80km$	0.79	0.18

Table 6: Mean and Standard Deviation of the R^2.

Window	**Mean Error** (%)	**Standard Error Deviation** (%)
$t_w = 2:45min$	8.1	19.7
$d_w = 80km$	2.0	8.2

Table 7: Mean and Standard Deviation of the relative error.

6 Conclusions

In this work, the Limo GT was successfully converted to use lithium ion batteries, increasing the range and the durability of the batteries. A data acquisition system to collect information concerning the position of the vehicle as well as the battery pack was successfully implemented, using a *Raspberry Pi* device.

The data collected was used to test range prediction methods to eliminate range anxiety. Several **trip-** and **history-based** methods were implemented.

In the **trip-based** models it was generally shown that the performance of all the models improved with the length of the segment considered. It was also concluded that the best performance was provided by the regression model. It was also seen that the performance of the statistical models gets worse as the dataset is reduced, while the physical models retain predictive capability even for small datasets.

Due to the fact that the altitude estimations were not reliable, the road slope estimations were not reliable. Because of this, it was not possible to accurately predict the instantaneous consumption of the vehicle, making the introduction of the efficiency of the electric motor impossible. However it was successfully extracted a efficiency map of the vehicle.

Two different formulations of history-based were also successfully implemented using methods based on the moving average algorithm. The first method considered a constant time window and the second a constant distance window. The results shown were compatible with commercial range prediction of vehicles.

References

[1] European Comission. Roadmap to a Single Europoean Transport Area - Towards a competitive and resource efficient system. 2011.

[2] International Energy Agency. Global EV Outlook 2020, 2020.

[3] Deloitte. 2018 Deloitte Global Automotive Consumer Study. pages 1–47, 2018.

[4] Christopher King, Wynita Griggs, Fabian Wirth, Karl Quinn, and Robert Shorten. Alleviating a form of electric vehicle range anxiety through on-demand vehicle access. *International Journal of Control*, 88(4):717–728, 2015.

[5] Achim Enthaler and Frank Gauterin. Method for reducing uncertainties of predictive range estimation algorithms in electric vehicles. *2015 IEEE 82nd Vehicular Technology Conference, VTC Fall 2015 - Proceedings*, pages 1–5, 2016.

[6] Maria Nilsson. Electric Vehicle: A range anxiety interview study. (November), 2011.

[7] Joonki Hong, Sangjun Park, and Naehyuck Chang. Accurate remaining range estimation for Electric vehicles. *Proceedings of the Asia and South Pacific Design Automation Conference, ASP-DAC*, 25-28-Janu:781–786, 2016.

[8] Christophe Moure, Marina Roche, and Marco Mammetti. Range estimator for electric vehicles. *2013 World Electric Vehicle Symposium and Exhibition, EVS 2014*, pages 1–15, 2014.

[9] Nicolas Denis, Maxime R. Dubois, Karol Angarita Gil, Thomas Driant, and Alain Desrochers. Range prediction for a three-wheel

plug-in hybrid electric vehicle. *2012 IEEE Transportation Electrification Conference and Expo, ITEC 2012*, pages 1–6, 2012.

[10] Luca Bedogni, Luciano Bononi, Alfredo D Elia, Marco Di Felice, Marco Di Nicola, and Tullio Salmon Cinotti. Driving Without Anxiety : a Route Planner Service with Range Prediction for the Electric Vehicles. *2014 International Conference on Connected Vehicles and Expo (ICCVE)*, pages 199–206, 2014.

[11] Chayada Chaiyamanon, Angkee Sripakagorn, and Nuksit Noomwongs. Dynamic modeling of electric tuk-tuk for predicting energy consumption in bangkok driving condition. *SAE Technical Papers*, 1, 2013.

[12] Christophe Moure, Marina Roche, and Marco Mammetti. Range estimator for electric vehicles. *2013 World Electric Vehicle Symposium and Exhibition, EVS 2014*, pages 1–15, 2014.

[13] Donkyu Baek, Yukai Chen, Alberto Bocca, Lorenzo Bottaccioli, Santa Di Cataldo, Valentina Gatteschi, Daniele Jahier Pagliari, Edoardo Patti, Gianvito Urgese, Naehyuck Chang, Alberto Macii, Enrico Macii, Paolo Montuschi, and Massimo Poncino. Battery-Aware operation range estimation for terrestrial and aerial electric vehicles. *IEEE Transactions on Vehicular Technology*, 68(6):5471–5482, 2019.

[14] Cedric De Cauwer, Maarten Messagie, Sylvia Heyvaert, Thierry Coosemans, and Joeri Van Mierlo. Electric vehicle use and energy consumption based on real world electric vehicle fleet trip and charge data its impact on existing EV research models. *World Electric Vehicle Journal*, 7(3):436–446, 2015.

[15] Lino Guzzella and Antonio Sciarretta. *Vehicle Propulsion Systems: Introduction to Modelling and Optimization*. Springer Berlin Heidelberg New York, 2013.

[16] Nectar Jinil and Sofana Reka. Deep Learning method to predict Electric Vehicle power requirements and optimizing power distribution. *5th International Conference on Electrical Energy Systems, ICEES 2019*, pages 1–5, 2019.

[17] Federica Foiadelli, Michela Longo, and Seyedmahdi Miraftabzadeh. Energy Consumption Prediction of Electric Vehicles Based on Big Data Approach. *Proceedings - 2018 IEEE International Conference on Environment and Electrical Engineering and 2018 IEEE Industrial and Commercial Power Systems Europe, EEEIC/I and CPS Europe 2018*, pages 1–6, 2018.

[18] Teng Liu, Xiaosong Hu, Shengbo Eben Li, and Dongpu Cao. Reinforcement Learning Optimized Look-Ahead Energy Management of a Parallel Hybrid Electric Vehicle. *IEEE/ASME Transactions on Mechatronics*, 22(4):1497–1507, 2017.

[19] Christoph Simonis and Roman Sennefelder. Route specific driver characterization for data-based range prediction of battery electric vehicles. *2019 14th International Conference on Ecological Vehicles and Renewable Energies, EVER 2019*, pages 1–6, 2019.

[20] A. D. Gordon, L Breiman, J. H. Friedman, R. A. Olshen, and C. J. Stone. Classification and Regression Trees. *Biometrics*, 40(3):874, sep 1984.

[21] Jan Dedek, Tomas Docekal, Stepan Ozana, and Tadeusz Sikora. BEV Remaining Range Estimation Based on Modern Control Theory - Initial Study. *IFAC-PapersOnLine*, 52(27):86–91, 2019.

[22] Lennon Rodgers, Daniel Frey, and Erik Wilhelm. Estimating an Electric Vehicle's Distance to Empty Using Both Past and Future Route Information. In *Proceding ASME 2013 international Design Engineering Technical Conferences and Computers and Information in Engineering Conference*, pages 1–9. American Society of Mechanical Engineers, aug 2013.

[23] Anastasia Bolovinou, Ioannis Bakas, Angelos Amditis, Francesco Mastrandrea, and Walter Vinciotti. Online prediction of an electric vehicle remaining range based on regression analysis. *2014 IEEE International Electric Vehicle Conference, IEVC 2014*, pages 1–8, 2014.

[24] Trevor Hastie, Robert Tibshirani, and Jerome Friedman. *The Elements of Statistical Learning*. Springer Series in Statistics. Springer New York, New York, NY, 2009.

[25] David Ruppert. *Statistics and Data Analysis for Financial Engineering*. Springer Texts in Statistics. Springer New York, New York, NY, 2011.